measured K_i values given above merely as approximations. It is noteworthy that at least one of the substances under study, **3**, inhibits mammalian as well as yeast decarboxylase.[2,3]

Acknowledgment. The studies were supported by NIH grants CA 11572 (to K.N.) and GM 22103 (to R.S.K.). We are grateful to Dr. F. Pilkiewicz, who was engaged in the initial stages of the difficult purification process, and to Mr. H. Naoki, Suntory Institute for Bioorganic Research, Osaka, for some of the NMR measurements.

References and Notes

(1) Calabresi, P.; Parks, R. E. In "The Pharmacologic Basis of Therapeutics", Goodman, L. S., Gilman, A., Eds., 5th ed.; MacMillan: New York, 1975; p 1253.
(2) A more detailed discussion of the biochemical properties, possible significance of these results, and implications for the prebiotic synthesis of pyrimidine ribotides will appear elsewhere: Potvin, B. W.; Stern, H. J.; Cooke, J. E.; Krooth, R. S.; Komura, H.; Nakanishi, K., unpublished work.
(3) Several other previously described compounds whose metabolites inhibit the decarboxylase have been shown to possess antineoplastic activity, e.g., Cadman, E. C.; Dix, D. E.; Hill, S. C.; Handschumacher, R. E. *Proc. Am. Assoc. Cancer Res.* **1976**, *17*, 208.
(4) The yeast orotidine 5′-monophosphate was purchased from Sigma Chemical Co., St. Louis, Mo.
(5) Formation of the product was first checked by incubating [2-^{14}C]barbituric acid with cold D-ribose 5-phosphate and monitoring the radioactivity which migrated with an R_f of 0.7 on a descending mode paper chromatograph (in contrast to the R_f of 0.39 for barbituric acid) (see ref 2). When yeast orotidine 5′-monophosphate decarboxylase and its substrate were present in an assay mixture containing barbituric acid, it was found that addition of a large excess of ribose phosphate resulted in maximal inhibition of enzyme activity by the earliest time point (5 min) which could be feasibly measured by the assay. The reaction conditions, however, were modified to those described, when it was found that excessive ribose phosphate led to unnecessary complications in the isolation procedure for product **1**.
(6) The K_m of the yeast orotidine 5′-monophosphate decarboxylase was 5.5×10^{-7} M. All K_i values were computed from double reciprocal plots using the method of least-squares regression analysis. While we can not rigorously prove that the observed inhibitions do not result from a breakdown of **1** (or **2**) into the known potent inhibitor **3** during the incubation period, we believe that this is unlikely for the following reasons. (1) The incubation was carried out at 37 °C for *30 min* at a *pH of 7.4*. It is doubtful that, under these conditions, adduct **3** could accumulate in sufficient quantity to account for the observed inhibition of enzyme activity (note that only a 0.1% yield of **2** and a trace of **3** were produced after incubating **1** for *1 week* at 37 °C at pH 5.5). (2) Whether the incubation was carried out at 4 or at 37 °C, the inhibition of enzyme activity did *not* increase with the time of incubation and was maximal at the earliest time point measured.
(7) D-Ribose and D-ribose 5-phosphate exhibit the following Cotton effects (in water), respectively: $\Delta\epsilon_{282} = -0.0006$ and $\Delta\epsilon_{280} = -0.019$. Note the very small $\Delta\epsilon$ values compared with the value of −0.20 for **1**; this shows that a larger proportion of **1** exists in the aldehydic form; the changes in $\Delta\epsilon$ values accompanying changes in concentration, pH, and buffer ionic strengths of solutions were minimal.
(8) The ^{13}C and ^{1}H chemical shifts were measured from external TSP.
(9) All NMR spectra were measured in D_2O, pD ~3.5, with JEOL FX-100 and Bruker WP-80 instruments. The β and α-anomeric carbons of ribose 5-phosphate appear at 102.0 and 97.2 ppm, respectively (3:1 ratio); the C-5 peaks also appear separately at 64.6 (β)/65.4 (α) ppm: Miwa, M.; Saito, H.; Sakura, H.; Saikawa, N.; Watanabe, F.; Matsushima, T.; Sugimura, T. *Nucleic Acid Res.* **1977**, *4*, 3997.
(10) The solubility of **1** in Me_2SO, DMF, THF, and MeCN was too low for NMR measurements.
(11) D-Ribose 5-phosphate has two ^{31}P NMR signals at 11.4–11.6 ppm, in D_2O. Chemical shifts are from H_3PO_4, the plus signs denoting downfield shifts from the reference.
(12) Fox, J. J.; Shugar, D. *Bull Soc. Chim. Belg.* **1952**, *61*, 44.
(13) The strong HDO solvent peak was removed by the partially relaxed Fourier transform technique.
(14) Since the pK_2' of the chromophore in **1** is ~6.5; it is in the neutral form.
(15) A possible mechanism for the genesis of adduct **1** is shown; since the optimum pH of the reaction was 5.5,[2] whereas the pK_a values of phosphate are ~1.5 and 6, and those of barbituric acid are 3.9 and 12.5, the reaction is depicted as proceeding through two monoanions. We thank Professor F. Ramirez for discussions. Other primary phosphate derivatives of sugars

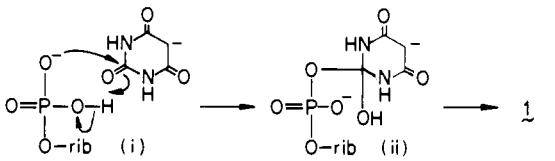

such as D-glyceraldehyde, D-ribulose, and four others reacted with barbituric acid under conditions similar to that of the formation of adduct **1**. For details see ref 2.
(16) The 5-methylene group, however, undergoes slow exchange. Thus the intensity of the 3.52-ppm 5-H peak is reduced to one half when the D_2O solution of **1** is left for 85 h at room temperature, pD 3.5, and then intensifies when **1** is further reprotonated for a period of 48 h. These changes however are accompanied by partial decomposition of the adduct.
(17) Harada, N.; Nakanishi, K. *Acc. Chem. Res.* **1972**, *5*, 257. Harada, N.; Chen, S.-M.L.; Nakanishi, K. *J. Am. Chem. Soc.* **1975**, *97*, 5345.
(18) The split CD of bis adduct **2** disappears upon leaving its aqueous solution for a few days. The inhibitory activity of the aqueous solution against orotidine 5′-monophosphate decarboxylase however *increases*. Although the minute quantity precluded direct chemical identification of the decomposition product(s), it is nearly certain that **2** had been converted into barbituric acid and its ribotide **3**, which has a higher K_i of $\sim 10^{-9}$ M.
(19) The intramolecular rearrangement is necessary to account for the spontaneous formation of the *N*-riboside linkage without prior activation of the ribose lactol function.
(20) A similar mechanism has been proposed in the biosynthesis of *N*-carboxybiotin: Kluger, R.; Adawadkar, P. D. *J. Am. Chem. Soc.* **1976**, *98*, 3741. We thank Professor D. Arigoni for bringing this to our attention.
(21) Whatman KC_{18} plate, developed with *i*-PrOH–H_2O (75:25 v/v). R_f values of adducts **1** and **4** were 0.66 and 0.80, respectively.
(22) We thank Dr. L. Johnson, Nicolet Instrument Corp., for this measurement at 200 MHz.
(23) Potvin, B. W.; Stern, H. J.; May, S. R.; Lam, G. F.; Krooth, R. S. *Biochem. Pharmacol.* **1978**, *27*, 655.
(24) Deceased Oct. 20, 1979.

H. Komura, K. Nakanishi*
Department of Chemistry, Columbia University
New York, New York 10027

B. W. Potvin, H. J. Stern, R. S. Krooth[24]
Department of Human Genetics and Development
College of Physicians and Surgeons, Columbia University
New York, New York 10032

Received September 4, 1979

Concerning the Role of Cyclopropene in the Allene to Propyne Isomerization. A Study of the Thermal Rearrangements of C_3H_3D Isomers[1]

Sir:

One of us[2] has recently suggested, on thermochemical kinetic grounds, that cyclopropene may be a possible intermediate in the thermal reversible isomerization of allene to propyne (methylacetylene) as shown in Scheme I. It was previously proposed[3] that this rearrangement occurred via a concerted process involving a direct 1,3-H shift. It is not possible to distinguish between these mechanisms with either unlabeled allene or propyne, since the stationary level of cyclopropene required by Scheme I is below the level of analytical detectability. However, alternative processes can *in principle* be distinguished by means of a study starting with deuteriopropyne. From propyne-*1*-d_1 (**1**), for instance, a concerted process would predict allene-d_1 (**3**) as the sole initial product. The mechanism via cyclopropene (Scheme II) on the other hand is likely to produce propyne-*3*-d_1 (**2**) in addition to allene-d_1. This is because the intermediate cyclopropene-*1*-d_1 (**4**) can revert to propyne-d_1 *in two ways* which are equivalent by symmetry (apart from the deuterium label) to produce **2** as well as **1**. This latter process is likely to be in effective competition with formation of **3** since it is known that cyclopropene isomerization favors the formation of propyne rather than allene.[4]

The necessary test materials were prepared as follows. **1** was made by reaction of propyne with ethylmagnesium bromide in THF solution at −50 °C, followed by hydrolysis with D_2O

Scheme I

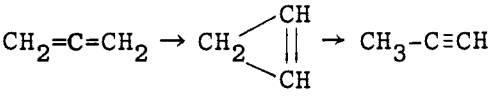

0002-7863/80/1502-1210$01.00/0 © 1980 American Chemical Society

Scheme II

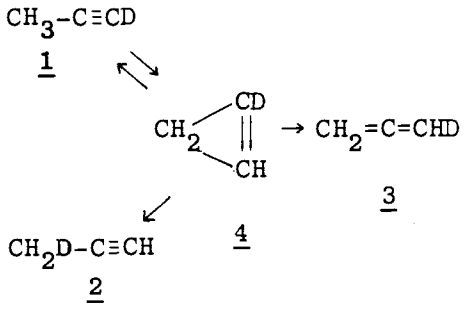

Scheme III

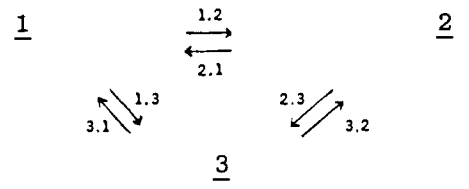

at 25 °C. After GC purification (6-m OPN column at 25 °C), **1** contained <0.4% **2**. **2** was made by reduction of 1-bromopropyne by $LiAlD_4$ in THF at 65 °C.[5] This procedure gave 12% **3** as well as 88% **2**. After GC purification, **2** contained <0.4% **1**. **3** was made by reaction of 1-chloropropyne with zinc and D_2O in dioxane at 100 °C.[6] GC purification of the initial product (80% **3** and 20% **2**) gave essentially pure **3**.

Pyrolyses of the C_3H_3D isomers were carried out in a quartz flow tube in the range 500–750 °C with a residence time of 32 s, using a low partial pressure of C_3H_3D in 1 atm of N_2. Products were frozen out and identified by GC, infrared, and mass spectral analysis. Below 650 °C only products **1**, **2**, and **3** could be observed (starting from any of the three pure isomers). Above 650 °C small quantities of methane and acetylene were also formed. A quantitative distribution of **1**, **2**, and **3** was obtained by IR analysis using bands which were uniquely attributable to each isomer, viz., at 3330 (≡C—H stretch of **2**), 2626 (≡C—D stretch of **1**), and 1960 cm^{-1} (C=C=C stretch of **3**). The results from a set of experiments starting from **1** are shown in Table I. They demonstrate how the C_3H_3D distribution essentially evolves from a pure component to an equilibrium mixture in a given time as the temperature is raised. Similar results were obtained starting from **2** and **3**.

A number of checks were carried out to establish that the processes involved were homogeneous first order and unimolecular in nature. When the tube was packed with glass wool [treated with *N,O*-bis(trimethylsilyl)acetamide], the same product distribution was obtained. Variation of the partial pressure of **1** (between ~1 and 37 Torr) did not affect the distribution, although at higher partial pressures there was some mass deficit. Mass spectral analysis of the product at 700 °C revealed <1% d_2- ($C_3H_2D_2$) and <5% d_0- (C_3H_4) containing products. This suggests that an atomic scrambling process is unimportant.

On the reasonably well-supported hypothesis that the C_3H_3D interconversions can be represented by a set of coupled unimolecular reactions (Scheme III), this kinetic scheme was solved by means of a matrix inversion technique for a set of trial rate constants. A complete set of optimal rate constants could be obtained on the assumption that their relative values did not change with temperature (i.e., they all had the same activation energy). Although this is unlikely to be exactly true, it is a reasonable approximation over a limited temperature range and any variation is probably masked by experimental scatter. In the optimal fit the rate constant ratios shown in Table II were found. These could be matched to the data at each temperature by a scaling factor to reproduce the experimental

Table I. Distribution of Products in Flow Pyrolysis of Propyne-1-d_1[a]

T, °C	1	2	3	other[b]
580	98.3	1.7	0	
600	96.7	2.9	0.4	
610	95.4	4.0	0.5	
620	93.9	5.3	0.8	
630	91.4	7.3	1.4	
640	87.6	10.6	1.7	
650	82.8	14.4	2.7	
660	78.2	18.3	3.5	
670	73.1	22.0	4.9	
680	60.4	30.5	9.1	
690	52.2	35.8	11.9	0.1
700	47.1	39.0	13.6	0.2
710	37.1	45.0	17.2	0.7
720	30.3	49.3	19.1	1.3
730	25.3	52.8	20.4	1.4
740	21.0	54.0	22.4	2.5
750	19.0	53.6	23.9	3.4
760	17.8	53.7	23.2	5.3

[a] Partial pressure of **1**, ~0.95 Torr. [b] $CH_4 + C_2H_2$.

Table II. Best-Fit Relative Rate Constants for Scheme III

process	rel k	process	rel k
1.2	1.00[a]	3.2	0.647
1.3	0.286	2.1	0.333
3.1	0.246	2.3	0.250

[a] Arbitrary.

conversion (from a given component). This produces, for instance, the rate constant sum, $k_{1,2} + k_{1,3}$, which fits the Arrhenius expression $\log (k_{1,2} + k_{1,3})/s^{-1} = (11.1 \pm 0.3) - (56.3 \pm 1.2)$ kcal $mol^{-1}/RT \ln 10$ (for the temperature range 600–740 °C).

From Table II, the important rate constant ratio $k_{1,2}/k_{1,3} = 3.5 \pm 0.5$ may be extracted.[7] That this is a reasonable finding can be seen by examining the low conversion ratio of **2:3** in Table I. This demonstrates clearly that **2** is formed more readily than **3** from **1**, and supports the contention that cyclopropene-1-d_1 is involved in these rearrangements. Formation of **2** from **1** appears to require the intermediacy of **4**. Whether or not formation of **3** also requires **4** as an intermediate depends on an analysis of the expected magnitude of $k_{1,2}/k_{1,3}$. This involves further assumptions about mechanism[7] and cannot be conclusively settled at this time. However, we estimate a value of 6.1 for this ratio based on the known behavior of cyclopropene[4,8] and estimates of isotope effects.[9] With the most pessimistic assumptions, this ratio is found not to vary by more than a factor of 2 and this therefore suggests that between 50 and 100% of the allene formed *does* come via the cyclopropene pathway.

Acknowledgment. We acknowledge the support of the Fonds der Chemischen Industrie (West Germany).

References and Notes

(1) Part 9 of Thermal Isomerisations. Part 8: L. Eisenhuth and H. Hopf, *Tetrahedron Lett.*, 1265 (1976).
(2) R. Walsh, *J. Chem. Soc., Faraday Trans. 1*, **72**, 2137 (1976).
(3) (a) A. Lifshitz, M. Frenklach, and A. Burcat, *J. Phys. Chem.*, **79**, 1148 (1975). (b) J. N. Bradley and K. O. West, *J. Chem. Soc., Faraday Trans. 1*, **71**, 967 (1975).
(4) I. M. Bailey and R. Walsh, *J. Chem. Soc., Faraday Trans. 1*, **74**, 1146 (1978).
(5) T. L. Jacobs, E. G. Teach, and D. Weiss, *J. Am. Chem. Soc.*, **77**, 6254 (1955).
(6) A. J. Morse and L. C. Leitch, *J. Org. Chem.*, **23**, 990 (1958).
(7) This ratio fits the data from ~15% total conversion up to equilibrium. There is some indication that at the lower temperatures (620–650 °C) it might be as high as 5.
(8) E. J. York, W. Dittmar, R. J. Stevenson, and R. G. Bergman, *J. Am. Chem. Soc.*, **95**, 5680 (1973).

(9) The complete solution to the cyclopropene mechanism is too complex to present here in detail and is delayed until a full paper. However, it takes explicit account of the intermediacy of both cyclopropene-1-d_1 (4) and cyclopropene-3-d_1. It also incorporates their relative propensities to shift H(D) and undergo degenerate rearrangement and all steps are considered potentially reversible. The particular ratio $k_{1,2}/k_{1,3}$ is given by $k_{1,2}/k_{1,3} = r_2/[r_1(1 + r_1 + r_2 + \alpha r_2)]$ where $r_1 = k_{4,3}/(k_{4,1} + k_{4,2})$ (Scheme II); r_2 = the relative propensity of the intermediate prop-1-ene-1,3-diyl biradical to reclose relative to H shift forming propyne; and $\alpha = k_H/k_D$, the primary kinetic isotope effect for all 1,2-H(D) shifts (secondary isotope effects being neglected).

(10) To whom correspondence can be addressed at the Institute für Organische Chemie der Universität Braunschweig, Schleinitzstrasse, D-3300 Braunschweig, West Germany.

H. Hopf,*[10] H. Priebe

Institut für Organische Chemie der Universität Würzburg Am Hubland, D-8700 Würzburg, West Germany

R. Walsh*

Department of Chemistry, University of Reading Whiteknights, Reading, Berks, RG6 2AD, England

Received September 14, 1979

Total Internal Reflection Raman Spectroscopy as a New Tool for Surface Analysis

Sir:

Attenuated total reflection infrared spectroscopy (ATR IR) has been established as a standard method for characterizing material surfaces.[1-5] The surface layer observable by the method, however, is fairly deep and far from such a thin surface layer that may control surface-sensitive properties. The penetration depth of the evanescent wave on total reflection is proportional to the wavelength of the incident light.[6] The wavelength of lasers (e.g., Ar 0.4880 μm) usually used for Raman spectroscopy is much shorter than those of infrared radiations (2.5-25 μm) concerned in infrared spectroscopy. Therefore, total internal reflection laser Raman spectroscopy, which deals with scattered light from the evanescent wave of a laser penetrating the sample, should give useful information on much thinner surface layers.

Applicability of total internal reflection to Raman spectroscopy was hinted by Harrick and Loeb.[7] Ikeshoji et al.[8] measured total internal reflection Raman spectrum of CS_2, by using a flint glass as the internal reflection element (IRE). The Raman signals were so weak and obscure that they needed time averaging of signals in real time and subsequent smoothing of the obtained spectra. Their failure to obtain distinct spectra seemed to be mainly due to the background of the IRE, for the low level of background is crucially important for recording the possibly very weak signals. We began to select a suitable material for the IRE to study feasibility of the total internal reflection Raman spectroscopy as a new tool for surface analysis, and found that the method is promising.

Sapphire has the least Raman background in the 800-1800-cm^{-1} range among the candidate materials with a refractive index >1.7, including flint glasses, TiO_2, and $SrTiO_3$. All the Raman peaks of sapphire that have a considerable intensity are located below 760 cm^{-1} and the background in the 800-3100-cm^{-1} range was <200 counts per second (cps) in the ordinary conditions, and sapphire was found the most appropriate for the IRE. Sapphire was cut into a plate with a side view of trapezoid, possessing 45 and 90° end face angles and the dimension 30 (c axis) × 10 × 1 mm, the surface for contact with a sample being the $(10\bar{1}0)$ plane. All the surfaces a laser beam hits were optically polished. The surface roughness was $<\lambda/10$.

Samples with a thin layer coating were prepared by coating polystyrene in various thicknesses on polyethylene films of 30-μm thickness. The polystyrene side of the sample was kept contacted intimately with the IRE surface with an appropriate pressure. The laser beam fell on the 45° end face of the IRE so that the refracted beam was incident onto the IRE-sample interface at an angle larger than the critical angle. The Raman scattering on total reflection was collected to the direction perpendicular to the IRE plate surface. The incident angle of laser onto the IRE-sample interface was varied from 68.5 to 64.8°, the latter being the critical angle for sapphire and polystyrene with a refractive index of 1.775[9] and 1.606,[9] respectively.

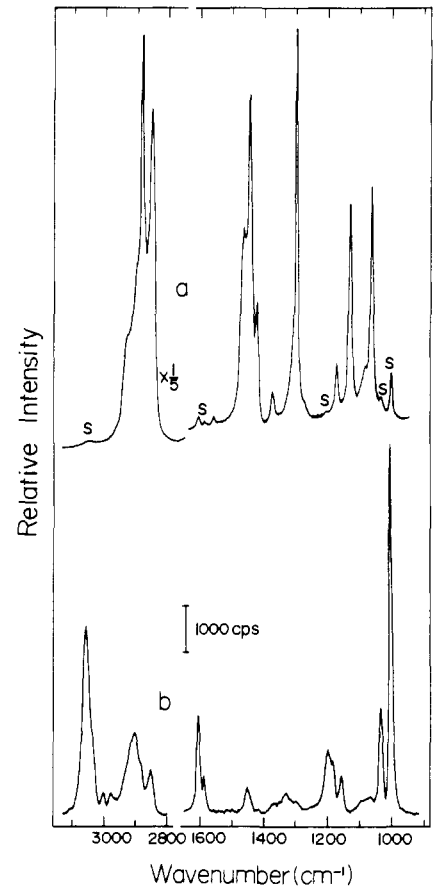

Figure 1. Raman spectra of a 30-μm-thick polyethylene film with an 1.1-μ-thick coating of polystyrene, measured by (a) illumination through the sample and (b) total internal reflection on the coated surface at an incident angle of 64.8°. The peaks marked S are due to polystyrene in the upper spectrum.

A laser Raman spectrometer used was Spex Ramalog 5 equipped with a Coherent Radiation argon ion laser CR-3 and a RCA-C31034 cooled photomultiplier. Total internal reflection Raman spectra were typically recorded with a 0.1- or 0.2-cm^{-1} s scanning speed, a time constant of 10 or 20 s, a 10-cm^{-1} slit width, and 200-mW laser power at 488.0 nm. The total internal reflection Raman spectra were measured on a single total reflection. The diameter of the laser beam was ~0.1 mm at the site of the total reflection.

The Raman spectrum measured by the conventional illumination through the polyethylene film with an 1.1-μm-thick coating of polystyrene (Figure 1a) shows several weak but distinct peaks due to polystyrene, the peak at 1002 cm^{-1} being the most intense of all the polystyrene peaks, in addition to predominant polyethylene peaks. Figure 1b is the total internal reflection Raman spectrum on the coated surface of the same sample. All the peaks therein are of polystyrene and even the strongest peaks of polyethylene at 2850 and 2890 cm^{-1} do not appear, showing striking contrast with the conventionally measured spectrum (Figure 1a). A total internal reflection

0002-7863/80/1502-1212$01.00/0 © 1980 American Chemical Society